



# 작약에서 소철괴사위축바이러스 및 오이모자이크바이러스의 검출을 위한 이중 프로브 기반 정량적 종합효소 연쇄반응 개발

승찬드라<sup>1</sup> · 키언찬초타<sup>2</sup> · 윤주연<sup>3,4,‡</sup> · 주호종<sup>5,6,7,8†</sup>

## Development of Duplex RT-qPCR Assay for the Simultaneous Detection of Cycas Necrotic Stunt Virus and Lychnis Mottle Virus in *Paeonia lactiflora*

Chandara Soeng<sup>1</sup>, Chanchota Kean<sup>2</sup>, Ju Yeon Yoon<sup>3,4,‡</sup>, and Ho Jong Ju<sup>5,6,7,8†</sup>

### ABSTRACT

Received: 2024 June 25  
1st Revised: 2024 July 22  
2nd Revised: 2024 August 13  
3rd Revised: 2024 August 20  
Accepted: 2024 August 20

This is an open access article distributed under the terms of the Creative Commons Attribution Non-Commercial License (<http://creativecommons.org/licenses/by-nc/3.0/>) which permits unrestricted non-commercial use, distribution, and reproduction in any medium, provided the original work is properly cited.

**Background:** In this study, a duplex probe-based reverse transcription quantitative polymerase chain reaction (RT-qPCR) assay was used to simultaneously detect Cycas necrotic stunt virus (CNSV) and Lychnis mottle virus (LycMoV) in *Paeonia lactiflora* (peony) collected from various locations in South Korea.

**Methods and Results:** CNSV and LycMoV infections were verified by using conventional RT-PCR using gene-specific primers. A high-precision quantification duplex probe-based qPCR assay was conducted on plasmid DNAs of target viruses and optimized to select the best-performing primers characterized by their ability to yield high relative fluorescence units and low cycle threshold values. Stable and consistent amplification plots and standard curves were achieved with primer and probe concentration of 0.25 μM and 0.2 μM, respectively, and an annealing temperature of 57°C. RT-qPCR was used with the selected primer sets and optimum conditions to detect the total RNA of peony leaves co-infected with CNSV and LycMoV. Successful detection occurred with a slightly weak sensitivity, having a detection limit of 10<sup>-3</sup> ng/μl.

**Conclusions:** The duplex probe-based RT-qPCR assay demonstrated in this study can improve the screening process for CNSV and LycMoV, leading to a reduction in the spread of these two plant viruses.

**Key Words:** *Paeonia lactiflora*, Cycas Necrotic Stunt Virus, Lychnis Mottle Virus, Reverse Transcription Quantitative Polymerase Chain Reaction



### INTRODUCTION

Peony is a perennial plant native to Central Asia and Southern Europe and is cultivated for ornamental and medicinal purposes. *Paeonia lactiflora*, famously known as Chinese peony, is a cut flower characterized by its vibrant flowers which represent wealth and nobleness.

Considered the king of flowers in the cut flower industry, it

is also known for its medicinal properties in traditional East Asian medicine, including tumor suppressive functions (Cheng *et al.*, 2011; Yue *et al.*, 2018).

A number of studies have been conducted on peonies in South Korea ranging from those on breeding, propagation, and micropropagation, as well as those on peony's medicinal properties (Ahn *et al.*, 2018; Im *et al.*, 2017; Lim *et al.*, 2013; Lim *et al.*, 2011; Yu, 1970).

<sup>†</sup>Corresponding author: (Phone) +82-63-270-2519 (E-mail) juhojong@jbnu.ac.kr

<sup>‡</sup>Co-corresponding author: (Phone) +82-63-270-4188 (E-mail) jyyoon@jbnu.ac.kr

<sup>1</sup>소<sup>1</sup>전북대학교 농생물학과 석사과정생 / Master's student, Department of Agricultural Biology, Jeonbuk National University, Jeonju 54896, Korea

<sup>2</sup>전북대학교 농생물학과 석사과정생 / Master's student, Department of Agricultural Biology, Jeonbuk National University, Jeonju 54896, Korea

<sup>3</sup>전북대학교 식물방역학과 부교수 / Associate Professor, Department of Plant Protection and Quarantine, Jeonbuk National University, Jeonju 54896, Republic of Korea

<sup>4</sup>전북대학교 농축산식품융합학과 부교수 / Associate Professor, Department of Agricultural Convergence Technology, Jeonbuk National University, Jeonju 54896, Korea

<sup>5</sup>전북대학교 농생물학과 교수 / Professor, Department of Agricultural Biology, Jeonbuk National University, Jeonju 54896, Korea

<sup>6</sup>전북대학교 식물방역학과 교수 / Professor, Department of Plant Protection and Quarantine, Jeonbuk National University, Jeonju 54896, Korea

<sup>7</sup>전북대학교 식물의학연구센터 교수 / Professor, Plant Medical Research Center, Jeonbuk National University, Jeonju 54896, Korea

<sup>8</sup>전북대학교 농업과학기술연구소 교수 / Professor, Institute of Agricultural Science and Technology, Jeonbuk National University, Jeonju 54896, Korea

Recent studies have shown that *P. lactiflora* is susceptible to viruses such as cycas necrotic stunt virus (CNSV, species: *Nepovirus cycas*, genus: *Nepovirus*, family: *Secoviridae*), lychnis mottle virus (LycMoV, species: *Stralarivirus lychnis*, genus: *Stralarivirus*, family: *Secoviridae*), tobacco rattle virus (TRV, species: *Tobravirus tabaci*, genus: *Tobravirus*, family: *Virgaviridae*), gentian kobu-sho associated virus (GKaV, genus: *Koshovirus* - unconfirmed), and amazon lily mild mottle virus (ALiMMV, species: *Amulavirus ALMMV*, genus: *Amulavirus*, Family: *Bromoviridae*) (Debat and Bejerman, 2023; Robertson *et al.*, 2009; Shaffer *et al.*, 2019; Shaffer *et al.*, 2022a; Shaffer *et al.*, 2021b; Uehara-Ichiki *et al.*, 2020; Yoon *et al.*, 2024).

Infection of CNSV showed symptoms of dwarfing and twisting on young leaves and leaving behind chlorotic or necrotic spots on mature leaves of *Cycas revoluta* (Kusunoki *et al.*, 1986). CNSV is known to infect alfalfa (Jiang *et al.*, 2019), Easter lily (Wylie *et al.*, 2012), and peony (Ochoa-Corona, 2003; Shaffer *et al.*, 2019; Tang *et al.*, 2020). In South Korea, CNSV was found to infect numerous other plants, including *Cnidium officinale* (Igori *et al.*, 2020), *Daphne odora*, and *Paeonia suffruticosa* (Lim *et al.*, 2019).

The infections are generally asymptomatic in peony cultivars. The vector responsible for spreading CNSV has not been identified yet, but the like of *Nepovirus* is well known for its capability to transmit via seed, pollens, sap inoculation, and nematodes (Shaffer *et al.*, 2019).

Yoo *et al.* (2015) thoroughly identified LycMoV genome organization. This virus is known to infect *Lychnis cognata* (Yoo *et al.*, 2015), *Rehmannia glutinosa* (Uehara-Ichiki *et al.*, 2016), *Vincetoxicum acuminatum* (Fujimoto *et al.*, 2018), *Paeonia lactiflora* (Shaffer *et al.*, 2019), *Angelica sinensis*, *Medicago sativa*, and *Prunus persica* (Jin *et al.*, 2023b). Infection of LycMoV in *A. sinensis* showed symptoms of leaf mosaic, chlorosis, yellow blotches, and mottling (Jin *et al.*, 2023b). LycMoV can be mechanically transmitted to *Catharanthus roseus* (Periwinkle), resulting in symptoms, such as chlorosis, stunting, rosette, and leaf curl (Shaffer *et al.*, 2019). Other means of LycMoV transmission include nematode transmission and transmission via propagation materials (Shaffer *et al.*, 2021a).

The presence of both CNSV and LycMoV in *P. lactiflora* has been reported in North America through high-throughput sequencing (HTS) analysis, and verified by using conventional RT-PCR. Shaffer *et al.* (2019) reported all peonies infected with LycMoV to be co-infected with CNSV. Jia *et al.* (2021)

performed HTS analysis of small RNA and mRNA of tree peonies exhibiting symptoms of yellowing, leaf rolling, stunted growth, and decline. CNSV and LycMoV were identified in mixed viral infections with other viruses such as apple stem grooving virus (ASGV), grapevine line pattern virus (GLPV), and three new viruses.

The population genetics of both CNSV and LycMoV were thoroughly studied through HTS analysis (Shaffer *et al.*, 2021a; Shaffer *et al.*, 2022b). Shaffer *et al.* (2022b) analyzed CNSV population genetics in an attempt to better understand virus epidemiology to improve diagnostic accuracy, and developed a multiplex RT-PCR assay to detect all published isolates of CNSV. Shaffer *et al.* (2021a) hypothesized that the introduction of LycMoV and other plant viruses to North America may be due to peony imports from Asia, and that the spread of LycMoV in the United States was due to propagation practices rather than vector-mediated transmission.

Jin *et al.* (2023a) established a detection system for LycMoV in *Angelica sinensis* by using a combination of a rapid colloidal gold immunochromatographic assay (GICA) with a reverse transcription loop mediated isothermal amplification assay (RT-LAMP), resulting in an assay with the sensitivity of  $2.53 \times 10^{-3}$  ng/ $\mu$ l.

Quantitative PCR (qPCR), being a fluorescence-based PCR, when coupled with high specificity of hydrolysis probe can be used as a highly sensitive virus screening tool capable of distinguishing the presence of multiple plant viruses simultaneously.

To fulfill the lack of a screening method for simultaneous detection of both viruses, this study demonstrated the application of a duplex hydrolysis probe-based RT-qPCR using the high precision quantification method for the detection of CNSV and LycMoV in *P. lactiflora*.

The study began from (1) detecting viruses by using conventional RT-PCR which were then confirmed through sequencing data, (2) using the dye-based qPCR for primer selection, (3) conducting standard curve comparisons between DNA and RNA standard templates, (4) optimizing the probe-based qPCR, and, finally, (5) establishing the duplex probe-based RT-qPCR.

## MATERIALS and METHODS

### 1. Plant materials and sample preparations

The symptomatic peony leaves were collected from fields

and kept in plastic bags. They were refrigerated at 4°C upon arrival in the laboratory, which was usually less than 6 hours after collection.

The total RNA was extracted from 50 mg of symptomatic leaves by using a filter-based spin basket method via the Plant RNA mini kit (Onsol, Suwon, Korea), following the manufacturer's instructions. RNA purity and quantity were acquired by using an Epoch Microplate Spectrophotometer (BioTek Instruments, Inc., Winooski, VT, USA).

The symptomatic samples were tested to determine the presence of opeony-infecting viruses, such as CNSV, LycMoV, TRV, ALiMMV, GKaV, citrus leaf blotch virus (CLBV), and cucumber mosaic virus (CMV) via conventional RT-PCR using the gene-specific primers derived from the published studies (Cardin *et al.*, 2010; Gress *et al.*, 2017; Robertson *et al.*, 2009; Shaffer *et al.*, 2022a; Shaffer *et al.*, 2021b).

The RT-PCR reaction was conducted by using the TOPscript™ RT-PCR kit (Enzynomics, Daejeon, Korea). The components consisted of 5 µl of TOPscript One-step RT-PCR kit, 0.5 µM of each primer, 1 µl of RNA, and water to a final reaction volume of 20 µl. The mixture was heated at 50°C for 30 minutes, which followed by 95°C for 10 minutes and 40 cycles 95°C for 30 seconds, 55°C for 30 seconds, and 72°C for 40 seconds, then finished with 72°C for 5 minutes.

Gel visualizations were conducted by using the Gel Doc

XR+ (Bio-Rad Laboratories Inc., Hercules, CA, USA) in 2% agarose gels electrophorized at 100 V for 35 minutes. All the isolated RNAs were then stored in -70°C freezer.

## 2. Primer and probe design

The sequencing data were obtained to aid in primer and probe design. The CNSV and LycMoV PCR products were ligated to pGEM-T Easy Vector (Promega Corporation, Madison, WI, USA), following the manufacturer's guidelines.

The competent cell of choice for the transformation was the DH5a chemically competent *E. coli* (Enzynomics, South Korea). Plasmid DNA purification was conducted by using the EZ-Pure Plasmid Prep Kit. Ver. 2 (Enzynomics, Daejeon, Korea). The plasmid DNAs were then sent for sequencing at BIONEER Inc. (Daejeon, Korea) and the sequencing data were then deposited in the GenBank database as LC785683 for the CNSV coat protein and LC785521 for the 412 bp-region of LycMoV.

Multiple sequence alignments were conducted by using the clustal omega tool provided by EMBL-EBI website (<https://www.ebi.ac.uk/jdispatcher/msa/clustalo>). qPCR primers and probes were selected in the conserved region of CNSV coat protein and LycMoV protease cofactor with the help of PrimerQuest tool provided free of use in Integrated DNA Technologies website (<https://idtdna.com/PrimerQuest/Home/Index>) and the sequencing data from BIONEER Inc.

**Table 1.** The RT-PCR and qPCR primers and probes used in the study to detect cycas necrotic stunt virus (CNSV) and lychnis mottle virus (LycMoV).

Target viruses	Purpose	Sequences 5' 3'	Primer size (mer)	Amplicon size (bp)	References	
CNSV	RT-PCR	F: CACCAAGTCCAGTTCTCTCTTATC	24	336	This study	
		R: CCACTCCTGTATCAGTATCAAC	22			
	qPCR	F: CAAAGTGTGGGAGAGGAGCTAC	22	102		
		R: GGGCAAGAACAAGTCCAAATC	21			
		Probe: FAM-ACCAAGTCCAGTTCTCTCGTATCCCT-BHQ1	26			
	Coat protein sequencing	F1: GCACATCAGGTCTTATTTGC	20	1500		This study
		R1: CCTTTGTGCTAGCAGCTGGCA	21			
F2: TGGGTGATATGAAGAGTGCT		20				
R2: GCTGAATGTGCTGTTCTTTACTCC		24				
LycMoV	RT-PCR	F: GGAGTCATGGCAAAGCTACG	20	412	Shaffer <i>et al.</i> , 2019	
		R: CAAGCACCTCAATTATTGCTCATC	25			
	qPCR	F: TGGCGTGGCTTACTTCAACC	19	112	This study	
		R: AGGATAGCCAGAGGAATACCC	21			
		Probe: Cy5-TGCTCCACAATTGCCTTCAATCCC-BHQ3	24			

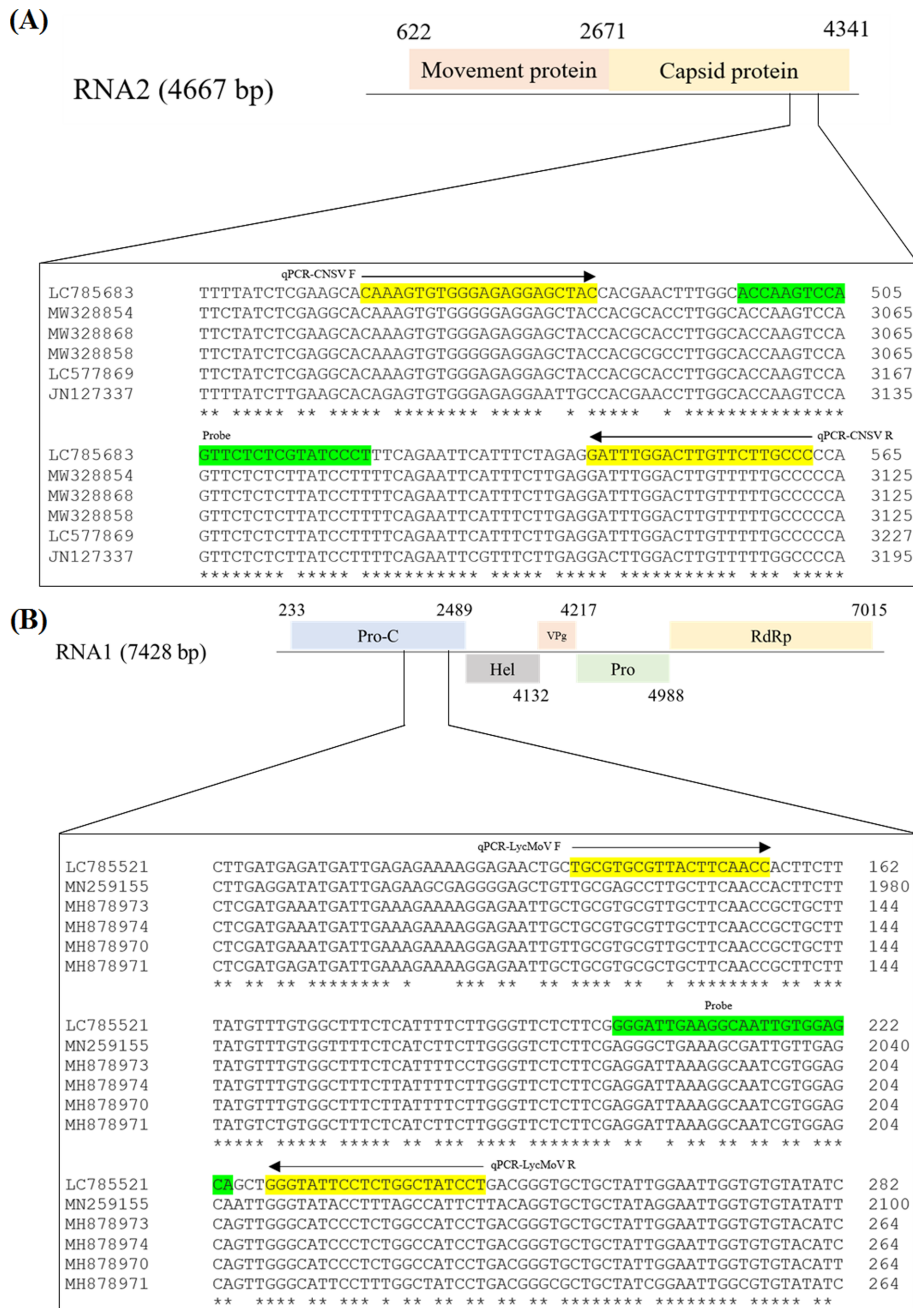


Fig. 1. qPCR Primer and probe location for the detection of CNSV (A) and LycMoV (B).

The CNSV qPCR primers and probe were selected from the multiple sequence alignment of LC785683, MW328854, MW328868, MW328858, LC577869, and JN127337. The LycMoV qPCR primers and probe were selected from the multiple sequence alignment of LC785521, MN259155, MH878973, MH878974, MH878970, and MH878971 (Table 1 and Fig 1). All isolates were retrieved from GenBank database.

### 3. Primer selection by using the dye-based qPCR

The dye-based qPCR was performed to select the best-performing primers, which produced a low Ct value and high fluorescence, for probe-based detection.

The reactions were conducted by using SYBR Green double-stranded DNA-binding dye via the TOPreal SYBR Green qPCR High-ROX PreMIX (Enzymomics, Daejeon, Korea) on the plasmid DNA of the corresponding target viruses. The

components consisted of 10  $\mu\text{l}$  of TOPreal qPCR 2  $\times$  PreMIX (SYBR Green with high ROX), 0.5  $\mu\text{M}$  of each primer, 1  $\mu\text{l}$  of DNA, and water to a final reaction volume of 20  $\mu\text{l}$ .

The mixture was heated at 95°C for 10 minutes and 40 cycles of 95°C for 10 seconds, 55°C for 15 seconds, and 72°C for 30 seconds. The melt curve analysis was conducted by heating the mixture to 65°C for 10 seconds and gradually increased to 95°C by 0.5°C/s.

These qPCR experiments were conducted in the CFX Opus 96 Real-Time PCR systems (Bio-Rad Laboratories Inc., Hercules, CA, USA). The CNSV primer set was selected from 26 CNSV primer sets targeting different regions of the CNSV genome. The LycMoV primer set was selected from 6 LyMoV primer sets targeting the Pro-C region of the LycMoV genome.

The best primer sets were selected based on having a low cycle threshold (Ct) value, high relative fluorescence units (RFU), and consistent standard curves and amplification plots. The primer specificity was assessed by performing dye-based qPCR using nucleic acids from four target viruses, which included CNSV, LycMoV, TRV, and GKaV.

#### 4. Comparisons of the standard curves by using the dye-based qPCR

Both the DNA and RNA standard curves were compared through high precision quantification using qPCR and RT-qPCR, respectively (Table 2).

The comparison was done to find the most suitable form of nucleic acids. The evaluation was conducted using CNSV as the viral target of interest. All of the nucleic acids were quantified twice using the Epoch Microplate Spectrophotometer (BioTek Instruments, Inc., Winooski, VT, USA). averaged, and diluted with nuclease free water to 1 ng/ $\mu\text{l}$ ; and then serially diluted to 10<sup>-7</sup> ng/ $\mu\text{l}$ . The dye-based qPCR with SYBR Green

dsDNA-binding dye was used for the evaluation. These experiments were conducted in duplicates using the StepOne Real-Time PCR system (Applied Biosystems, Foster City, CA, USA).

Circular plasmid DNA and linearized plasmid DNA were used for the DNA standard curves. Circular plasmid DNA was linearized by using a restriction enzyme carefully selected from the vector map of pGEM-T Easy Vector with the aid of the sequencing data of the said amplicon to avoid cleaving the target of interest. Total RNA and transcript RNA were used for the RNA standard curves. The total RNA was obtained by using filter-based spin basket method. The transcript RNA was synthesized via in vitro transcription using the MEGAscript T7 Transcription kit (Thermo Fisher Scientific, Waltham, MA, USA).

#### 5. Optimizations of the probe-based qPCR

The probe-based qPCR was performed to assess the primer and probe specificity among CNSV and LycMoV by using the TOPreal Multi-Probe qPCR PreMIX (Enzynomics, Daejeon, Korea). The components consisted of 10  $\mu\text{l}$  of TOPreal qPCR 2  $\times$  PreMIX (TaqMan Probe for multiplex), 0.2  $\mu\text{M}$  of probe, 0.5  $\mu\text{M}$  of each primer, 1  $\mu\text{l}$  of DNA, and water to a final reaction volume of 20  $\mu\text{l}$ . The mixture was heated at 95°C for 10 minutes and then 40 cycles of 95°C for 10 seconds and 55°C for 30 seconds.

The parameters for reaction optimization included primer and probe concentrations, annealing temperatures, and detection limit. The optimum condition was decided based on the stability of the amplification plot, low Ct value, and similarly RFU. The RFU became a factor in the optimizations due to the duplex experiment requiring similar fluorescence levels from both targets.

The primer and probe concentrations included 0.5  $\mu\text{M}$ , 0.25  $\mu\text{M}$ , and 0.05  $\mu\text{M}$  primers combined with 0.2  $\mu\text{M}$ , 0.1  $\mu\text{M}$ , and 0.05  $\mu\text{M}$  probes. The best combination was then selected for

**Table 2.** Comparison of standard curves to select the best template for the high precision quantification dye-based qPCR using the standard curve experiments.

Types of qPCRs	Types of templates			
	DNA template		RNA template	
	Circular plasmid	Linearized plasmid	Total RNA	Transcript RNA
	qPCR	qPCR	RT-qPCR	RT-qPCR
Kits	TOPreal SYBR Green qPCR High-ROX PreMIX	TOPreal SYBR Green qPCR High-ROX PreMIX	TOPreal SYBR Green RT-qPCR High-ROX Kit	TOPreal SYBR Green RT-qPCR High-ROX Kit
Method used to produce the templates	pGEM-T Easy Vector	pGEM-T Easy Vector linearized by using restriction enzyme	Filter-based spin basket isolation (total RNA isolation)	MEGAscript® T7 Transcription Kit (in vitro transcription)

These experiments were conducted in duplicates by using the StepOne Real-Time PCR system (Foster City, CA, USA).

the next optimization stage which is the annealing temperature test that included 63°C, 61°C, 59°C, 57°C, 55°C, and 53°C. The best combination was selected for the detection limit test using the plasmid DNA with the concentrations ranging from 1 ng/μl to 10<sup>-7</sup> ng/μl.

These qPCR experiments were conducted in the CFX Opus 96 Real-Time PCR systems (Bio-Rad Laboratories Inc., Hercules, CA, USA).

## 6. Application of the duplex probe-based RT-qPCR

The duplex RT-qPCR reaction was conducted by using the TOPreal Multi-Probe RT-qPCR kit (Enzynomics, Daejeon, Korea).

The primer concentration, probe concentration, and annealing temperature were obtained from the duplex probe-based qPCR optimization experiments. The reaction components consisted of 5 μl of TOPreal One-step RT qPCR kit (TaqMan Probe for multiplex), 0.2 μM of each probe, 0.25 μM of each primer, 1 μl of RNA, and water to a final reaction volume of 20 μl.

The mixture was heated at 50°C for 30 minutes, then 95°C for 10 minutes, and 40 cycles 95°C for 5 seconds and 57°C for 30 seconds.

These qPCR experiments were conducted in the CFX Opus 96 Real-Time PCR systems (Bio-Rad Laboratories Inc., Hercules, CA, USA).

## RESULTS

### 1. Virus detection by using RT-PCR and verification through the sequencing data

The leaf sample infected with CNSV showed symptoms of mottle and chlorotic spots (Fig. 2A), while the leaf co-infected with CNSV and LycMoV showed chlorotic spots and wrinkles which expanded from the leaf base to the leaf end (Fig. 2B).

The presence of both CNSV and LycMoV were confirmed through RT-PCR resulting in amplicon size of 336 bp for CNSV and 412 bp for LycMoV (Fig. 2C).

BLAST analyses of acquired sequences confirmed the presence of CNSV and LycMoV. Our CNSV CP isolate shared a 91.54% similarity to another CNSV isolate from peonies in the United States (MW328854), a 91.26% identity with another CNSV isolate from Korean peony (LC577869), a 90.42% similarity with another CNSV isolate from lily (JN127337), and a 90.43% similarity with CNSV reference sequence derived from cycas (NC\_003792).

Our LycMoV isolate shared an 86.34% similarity with

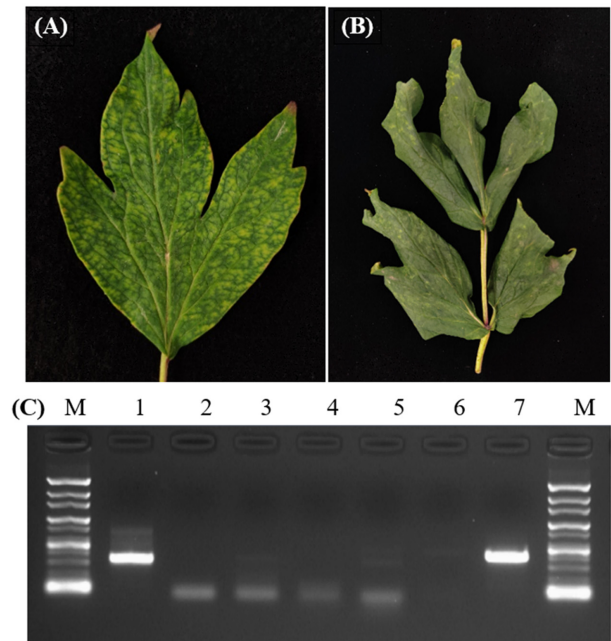


**Fig. 2. Collection of the symptomatic peony leaves and the detection of peony-infecting viruses by using conventional RT-PCR.** (A) the cycas necrotic stunt virus (CNSV) infected leaf. (B) the CNSV and lycnis mottle virus (LycMoV) co-infected leaf. (C) the RT-PCR results from the co-infected leaf in (B). 1 = CNSV: 336 bp, 2 = tobacco rattle virus (TRV: 328 bp), 3 = amazon lily mild mottle virus (ALiMMV: 590 bp), 4 = citrus leaf blotch virus (CLBV: 281 bp), 5 = cucumber mosaic virus (CMV: 657 bp), 6 = gentian kobusho associated virus (GKaV: 574 bp), 7 = LycMoV: 412 bp, and M = 100 bp marker.

another secovirus isolate from peony in China (MN259155) and a 93% similarity with another LycMoV isolate from peony in the United States (MH878973).

### 2. Primer selection by using the dye-based qPCR

Selected CNSV and LycMoV primer sets were specific to their own target virus in the form of circular plasmid DNA (Table 1).

Neither the amplification peak nor the Ct value was produced from the non-target DNA (Fig. 3A and Fig. 3C). The melt curve assay showed a sole peak, indicating the specificity of both primer sets (Fig. 3B and Fig. 3D). Negative controls being ultra pure water (Enzynomics, Daejeon, Korea) were undetectable in all cases, reinforcing the certainty that all the reactions were performed well.

### 3. Comparisons of the standard curves by using the dye-based qPCR for CNSV

The amplification data for each template targeting CNSV

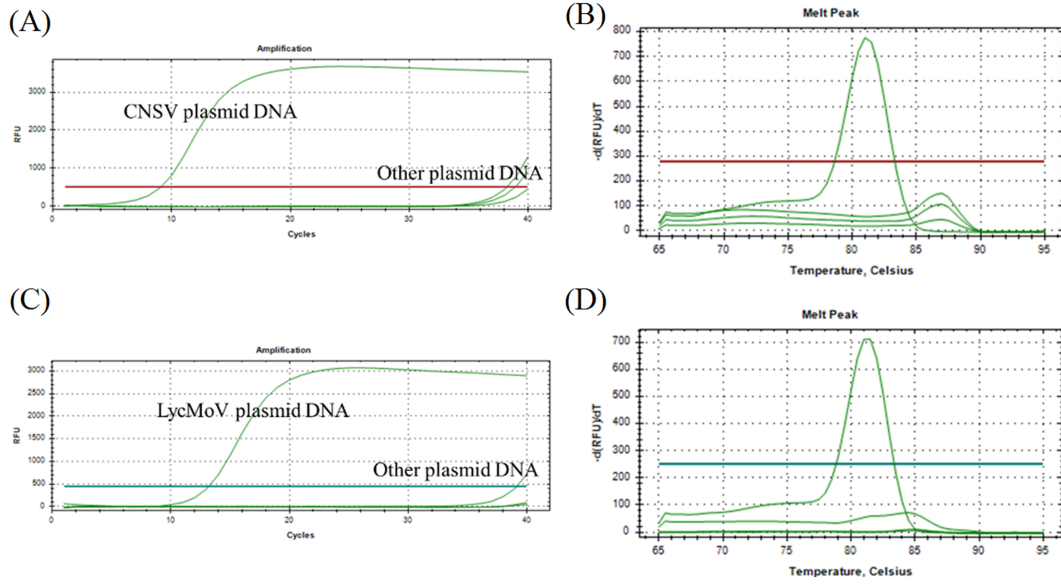


**Fig. 3. Specificity of CNSV and LycMoV qPCR primers confirmed by using dye-based qPCR.** Sole amplification plots of CNSV primer (A) and LycMoV primer (C) were obtained from amplifying artificially made mixture of CNSV, LycMoV, TRV, and GKAV plasmid DNAs. Melt curve analysis showed a single peak from CNSV PCR product (B) and from LycMoV PCR product (D). The primer concentration was 0.25  $\mu\text{M}$  and the annealing temperature was 55°C. These experiments were conducted in CFX Opus 96 Real-Time PCR systems (Bio-Rad Laboratories Inc., Hercules, CA, USA)

**Table 3.** The amplification data (mean Ct value) of the different types of templates produced within the range of 1  $\text{ng}/\mu\text{l}$  to  $10^{-7}$   $\text{ng}/\mu\text{l}$ .

Quantity ( $\text{ng}/\mu\text{l}$ )	Mean Ct value							
	DNA template				RNA template			
	Circular plasmid	SD	Linearized plasmid	SD	Total RNA	SD	Transcript RNA	SD
1	7.371285	0.02	4.152771	0.05	21.7316	0.05	22.78104	0.07
$10^{-1}$	10.98652	0.04	8.159449	0.05	27.08916	0.21	26.67378	0.2
$10^{-2}$	14.67084	0.08	12.9701	0.02	31.85391	0.75	33.13015	0.17
$10^{-3}$	17.68555	0.01	17.55114	0.06	35.84479	-	35.323	-
$10^{-4}$	22.49335	0.17	21.65792	0.01	34.83543	-	Undetermined	-
$10^{-5}$	26.85077	0.16	26.30221	0.04	35.86761	-	34.73265	-
$10^{-6}$	30.54506	0.23	32.54072	0.27	34.80863	-	Undetermined	-
$10^{-7}$	37.11721	-	37.75296	1.86	Undetermined	-	Undetermined	-

The DNA templates were circular plasmid and linearized plasmid. The RNA templates were total RNA and transcript RNA. The target of interest was cyas necrotic stunt virus (CNSV) being amplified by using CNSV qPCR primer (102 bp). The primer concentration was 0.5  $\mu\text{M}$ , and the annealing temperature was 55°C. These experiments were conducted in duplicates by using the StepOne Real-Time PCR system (Applied Biosystems, Foster City, CA, USA).

was shown in Table 3. Experiments were conducted in duplicates, resulting in a mean Ct value. At the highest concentration of 1  $\text{ng}/\mu\text{l}$ , the DNA templates showed the lowest Ct value compared to RNA templates, in which the lowest Ct value was from the linearized plasmid at 4.15. At the lowest concentration of  $10^{-7}$   $\text{ng}/\mu\text{l}$ , the DNA templates were still detectable, whereas the RNA templates could no longer be determined. Although the linearized plasmid had lower Ct value at the highest concentration

compared to the circular plasmid, as the concentration kept getting lower, specifically after 3 times of 10-fold serial dilution at  $10^{-3}$   $\text{ng}/\mu\text{l}$ , the Ct value of both templates matched for the rest of the dilutions. For the RNA templates, the detectable range was  $10^{-3}$   $\text{ng}/\mu\text{l}$  because the Ct values of RNA templates after  $10^{-3}$   $\text{ng}/\mu\text{l}$  were either inconsistent or undetermined, indicating that the fluorescence signals were unstable and unreliable.

This inaccuracy was observed through the standard curve in

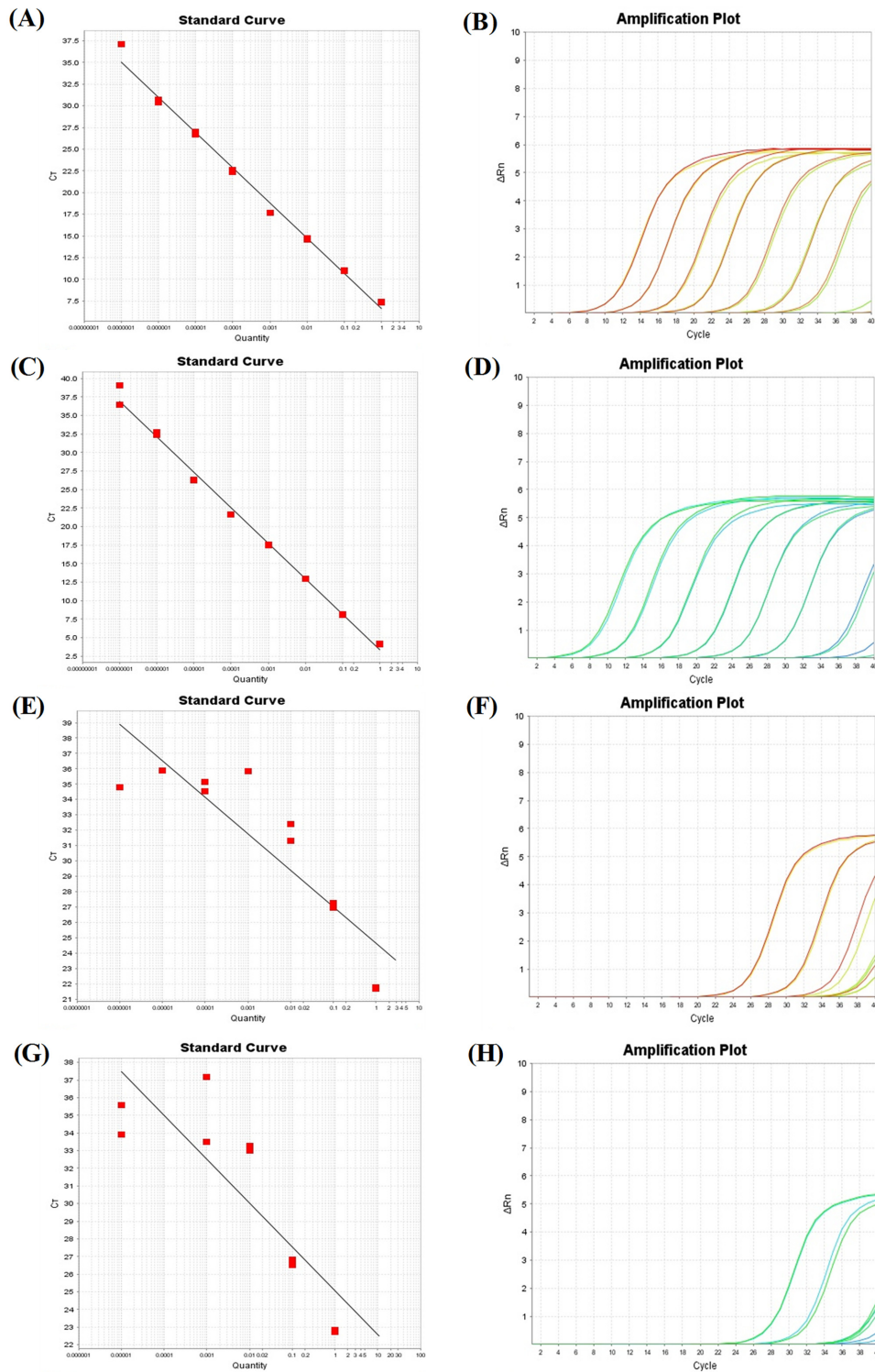


**Fig. 4.** The standard curves and amplification plots (linear graph) of the different standard templates targeting CNSV within the range of  $1 \text{ ng}/\mu\text{l}$  to  $10^{-7} \text{ ng}/\mu\text{l}$ . Standard curves of (A) the circular plasmid ( $R^2 = 0.992$ ), (C) the linearized plasmid ( $R^2 = 0.995$ ), (E) the total RNA ( $R^2 = 0.781$ ), and (G) the transcript RNA ( $R^2 = 0.722$ ). Amplification plots of (B) the circular plasmid, (D) the linearized plasmid, (F) the total RNA, and (H) the transcript RNA. The primer concentration was  $0.5 \mu\text{M}$  and the annealing temperature was  $55^\circ\text{C}$ . These experiments were conducted in the StepOne Real-Time PCR system (Applied Biosystems, Foster City, CA, USA).



which the  $R^2$  value of the total RNA template was only 0.781 while the transcript RNA template was 0.722, both of which were not close to 1, enforcing the claim that the detection limit of the RNA templates were  $10^{-3}$  ng/ $\mu$ l (Fig. 4E and Fig. 4G).

For the DNA templates, on the other hand, the  $R^2$  value of the circular plasmid was 0.992 and the linearized plasmid was 0.995, both of which were close to 1, indicating a very high accuracy (Fig. 4A and Fig. 4C).

Based on the amplification plots, DNA templates produced equally spaced plots from the early stage of the amplification cycles, which were more desirable than amplification plots produced by RNA templates which were at the later stage of the amplification cycles.

Due to the similar performance of the circular plasmid and the linearized plasmid, the circular plasmid was the template of choice for the probe-based qPCR experiments.

#### 4. Optimizations for the probe-based qPCR

The selected primers were compatible with their hydrolysis probes, and their specificities corresponded to their targets (Fig. 5).

Primer concentration of 0.25  $\mu$ M, probe concentration of 0.2  $\mu$ M, and annealing temperature of 57°C were found to produce the best results, as well as decent RFU (Table 4 and 5). The templates for the standard curve construction were artificially made plasmid DNA mixture with the range from 1 ng/ $\mu$ l to  $10^{-7}$  ng/ $\mu$ l. The  $R^2$  value for the CNSV slope was 0.998, while the LycMoV slope was 0.993, indicating a high accuracy (Fig. 6A). The detection limit was  $10^{-6}$  ng/ $\mu$ l for both viruses. The negative control was undetectable for both sets of primers. The selected primers from the dye-based qPCR functioned properly,

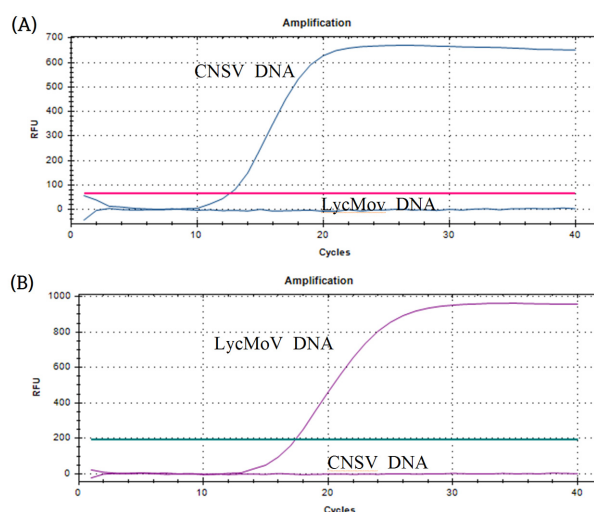


**Fig. 5. Primer and probe specificity of qPCR primers and probes for probe-based RT-qPCR experiments.** (A) CNSV primers and probe were used to amplify artificially made mixture of CNSV and LycMoV plasmid DNA. (B) LycMoV primers and probe were used to amplify artificially made mixture of CNSV and LycMoV plasmid DNA. The primer concentration was 0.5  $\mu$ M, the probe concentration was 0.2  $\mu$ M, and the annealing and elongation temperature was 55°C. These experiments were conducted in CFX Opus 96 Real-Time PCR systems (Bio-Rad Laboratories Inc., Hercules, CA, USA)

while the Ct values were almost identical. When the RFU values from the dye-based qPCR (Fig. 6B and Fig. 6D) and from the probe-based qPCR (Fig. 6B and Fig. 6C) were compared, there was a noticeable drop for both targets.

#### 5. The application of the duplex probe-based RT-qPCR

The optimum conditions of a primer concentration of 0.25  $\mu$ M,

**Table 4.** Optimization of the primer concentration for the duplex probe-based qPCR for the detection of cycas necrotic stunt virus (CNSV) and lychnis mottle virus (LycMoV).

Pri. Con. <sup>1)</sup> ( $\mu$ M)	Pro. Con. <sup>2)</sup> ( $\mu$ M)	Ct value (ng/ $\mu$ l)										Highest RFU	
		1		$10^{-1}$		$10^{-2}$		$10^{-3}$		$10^{-4}$		CNSV	LycMoV
0.5	0.2	12.60	17.35	16.66	20.76	21.50	25.30	26.84	30.45	30.69	34.07	674	960
	0.1	13.34	16.14	17.17	19.83	22.19	24.54	27.53	29.70	31.09	32.98	562	643
	0.05	12.18	14.16	16.32	18.20	21.24	23.03	26.61	27.99	30.00	31.88	362	157
0.25	0.2	13.37	16.34	17.22	19.86	22.05	24.50	27.53	29.75	31.12	32.98	804	956
	0.1	12.99	16.11	17.10	19.81	22.07	24.42	27.35	29.19	31.01	32.44	534	621
0.05	0.05	12.40	15.44	16.46	19.10	21.38	24.10	25.71	28.24	30.45	32.17	214	171
	0.05	11.98	14.47	16.69	19.16	21.87	23.43	27.46	27.10	31.73	32.34	207	151

<sup>1)</sup>Pri. Con.; primer concentration ( $\mu$ M). <sup>2)</sup>Pro. Con.; probe concentration ( $\mu$ M). The tested primer concentrations were 0.5  $\mu$ M, 0.25  $\mu$ M, and 0.05  $\mu$ M. The tested probe concentrations were 0.2  $\mu$ M, 0.25  $\mu$ M, and 0.05  $\mu$ M. The standard curve had 5 magnitudes ranging from 1 ng/ $\mu$ l to  $10^{-4}$  ng/ $\mu$ l. These experiments were conducted in the CFX Opus 96 Real-Time PCR systems (Bio-Rad Laboratories Inc., Hercules, CA, USA).

**Table 5.** Optimization of the annealing temperature for the duplex probe-based qPCR for the detection of cycas necrotic stunt virus (CNSV) and lycnis mottle virus (LycMoV).

Pri : Prob Con <sup>1)</sup> ( $\mu\text{M}$ )	Temp. <sup>2)</sup> ( $^{\circ}\text{C}$ )	Ct value ( $\text{ng}/\mu\text{l}$ )										Highest RFU	
		1		$10^{-1}$		$10^{-2}$		$10^{-3}$		$10^{-4}$		CNSV	LycMoV
		CNSV	LycMoV	CNSV	LycMoV	CNSV	LycMoV	CNSV	LycMoV	CNSV	LycMoV		
0.25 : 0.2	63	11.20	15.14	15.70	18.50	21.14	23.96	26.19	29.24	28.50	31.33	682	650
	61	12.11	15.83	16.18	19.23	22.35	24.88	26.64	29.27	29.64	32.20	770	760
	59	13.31	16.06	17.22	19.75	23.08	25.36	27.96	30.21	31.16	33.00	884	895
	57	12.86	16.59	17.01	20.21	22.72	25.74	27.98	30.69	31.09	33.21	965	1042
	55	13.37	16.34	17.22	19.86	22.05	24.50	27.53	29.75	31.12	32.98	804	956
	53	13.19	18.29	18.32	21.18	24.26	26.93	29.41	31.96	32.49	34.50	922	1113

<sup>1)</sup>Pri : Prob Con; primer : probe concentration ( $\mu\text{M}$ ). <sup>2)</sup>Temp; temperature ( $^{\circ}\text{C}$ ). The tested annealing temperature were  $63^{\circ}\text{C}$ ,  $61^{\circ}\text{C}$ ,  $59^{\circ}\text{C}$ ,  $57^{\circ}\text{C}$ ,  $55^{\circ}\text{C}$ , and  $53^{\circ}\text{C}$ . The standard curve has 5 magnitudes ranging from  $1 \text{ ng}/\mu\text{l}$  to  $10^{-4} \text{ ng}/\mu\text{l}$ . These experiments were conducted in the CFX Opus 96 Real-Time PCR systems (Bio-Rad Laboratories Inc., Hercules, CA, USA).

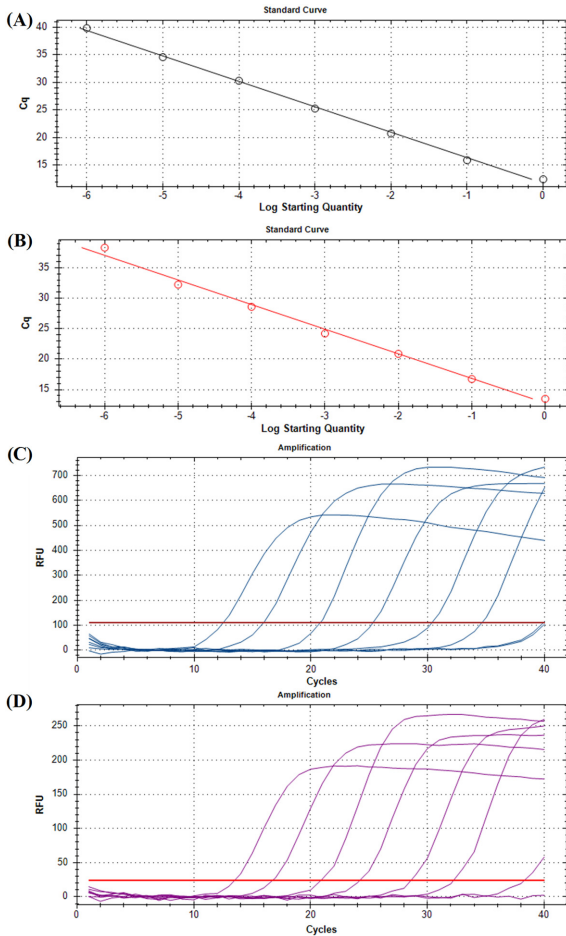


**Fig. 6.** The standard curve, amplification plot, and detection limit of the optimized duplex probe-based qPCR assay conducted on cycas necrotic stunt virus (CNSV) and lycnis mottle virus (LycMoV) circular plasmid DNAs. The primer concentration was  $0.25 \mu\text{M}$ . The probe concentration was  $0.2 \mu\text{M}$ . The annealing temperature was  $57^{\circ}\text{C}$ . The standard range was from  $1 \text{ ng}/\mu\text{l}$  to  $10^{-7} \text{ ng}/\mu\text{l}$ . The standard curve of CNSV (black)(A) and LycMoV (red)(B). The amplification plot of CNSV(C) and LycMoV(D).

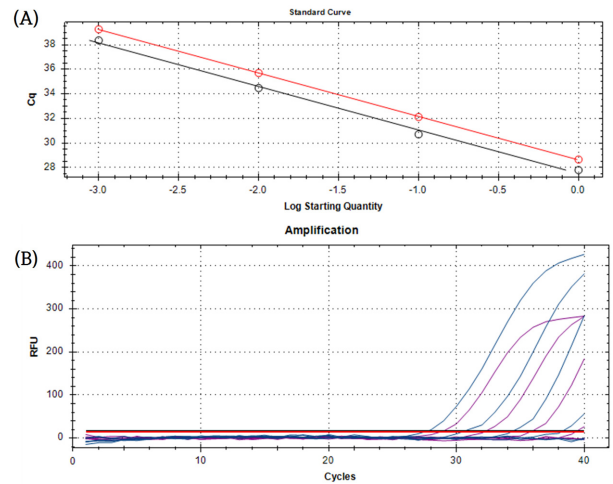


**Fig. 7.** The standard curve, amplification plot, and detection limit of the duplex probe-based RT-qPCR assay conducted on cycas necrotic stunt virus (CNSV) and lycnis mottle virus (LycMoV) total RNA. (A) Amplification plot and (B) standard curve of simultaneous detection of cycas necrotic stunt virus (CNSV) and lycnis mottle virus (LycMoV) total RNAs. The primer concentration was  $0.25 \mu\text{M}$ . The probe concentration was  $0.2 \mu\text{M}$ . The annealing temperature was  $57^{\circ}\text{C}$ . These were the same conditions derived from the optimized duplex probe-based qPCR experiment. The standard range was from  $1 \text{ ng}/\mu\text{l}$  to  $10^{-4} \text{ ng}/\mu\text{l}$ . The standard curve of CNSV target had an  $R^2$  value of 0.996, while LycMoV target had an  $R^2$  value of 1. The qPCR efficiencies were 91.5% for CNSV primer sets and 91.7% for LycMoV primer sets.

a probe concentration of  $0.2 \mu\text{M}$ , and an annealing temperature at  $57^{\circ}\text{C}$  were applied to detect CNSV and LycMoV in the form of total RNA by using the duplex probe-based RT-qPCR. While the detection was possible, the assay was slightly less sensitive than qPCR (Fig. 7).

The  $R^2$  value of the CNSV slope was 0.985 and the LycMoV slope was 1, graphed as a 4-magnitude standard curve. The detection limit was  $10^{-3} \text{ ng}/\mu\text{l}$  for both viruses. The qPCR efficiencies were

91.5% for CNSV primer and 91.7% for LycMoV (Fig. 7A). The negative control was undetectable for both sets of primers.

## DISCUSSIONS

Based on recent studies, *P. lactiflorais* known to be infected to numerous several plant viruses, including CMV, CLBV, TRV, LycMoV, GKaV, ALiMMV, and CNSV, which can cause economic harm to production of *P. lactiflorais* (Cardin et al., 2010; Gress et al., 2017; Robertson et al., 2009; Shaffer et al., 2019; Shaffer et al., 2022a; Shaffer et al., 2022b). Therefore, sensitive and accurate diagnosis is essential for effective management in the field and quarantine conditions.

The application of qPCR technology in the field of plant disease diagnostic results in a big leap of possibilities thanks to its powerful and sensitive diagnostic capabilities with increased accuracy and scalability that can be adopted into many biomolecular experiments and is shown to be superior to many current and previously adopted techniques. Nonetheless, there remain distinct parameters that can heavily influence the results produced from qPCR experiments. Experiments performed on the same sample can, in the worst cases, result in statistically different values of target quantity or copy number (Smith et al., 2006).

While a number of methods have been developed for the detection of either CNSV or LycMoV in peonies (Jia et al., 2021; Shaffer et al., 2019; Shaffer et al., 2021a; Shaffer et al., 2022b). However, a detection method taking advantage of the high sensitivity and specificity of qPCR has not been established yet until this study. Here, we report the successful development of duplex probe-based RT-qPCR assay to detect two viruses infecting peonies, CNSV or LycMoV. The sensitivity of the optimized duplex RT-qPCR assay was comparable to a study that used GICA-RT-LAMP to detect LycMoV in *A. sinensis* (Jin et al., 2023a). Due to the difficulty in acquiring suitable total RNAs with sufficient quality for qPCR experiments, most developments (Fig. 3 to Fig. 6) were conducted using cloned circular plasmid DNA of target virus which was thoroughly studied among DNA and RNA standard templates because of the stability and reproducibility (Pfaffl, 2004).

The dye-based qPCR experiment on plasmid DNA of target viruses was primarily used for primer selection. The probe-based qPCR experiment on plasmid DNA of target viruses was mainly used for the assay optimization, resulting in the use of 0.25  $\mu$ M primer and 0.2  $\mu$ M probe for both viral primer sets coupled with an annealing temperature of 57°C. These settings

were then applied and optimized to the duplex probe-based RT-qPCR assay of the total RNA of target viruses which resulted in the first successful utilization of RT-qPCR as a screening method for two peony viruses, being CNSV and LycMoV, with the detection limit of  $10^{-3}$  ng/ $\mu$ l.

This RT-qPCR assay can be improved further by using a more specific RNA extraction method tailored to the samples containing high secondary metabolites like peonies or by purifying the standard templates which can result in a more accurate Ct value.

Although there exist previous studies which involved viral RNA extraction from peony leaves, none of them were intended for qPCR experiments; therefore, further studies need to be conducted focusing on viral RNA extraction method from peony samples that produce RNA suitable for qPCR experiments (Jia et al., 2021; Lim et al., 2019; Shaffer et al., 2021a; Shaffer et al., 2022b).

Another limitation of standard template preparation which is usually overlooked is the need for standard templates quantification via a separate instrument, for example spectrophotometric measurements or fluorometric measurements. Measurement of samples with low impurity would lead to incorrect quantity of target nucleic acids.

Beinhauerova et al. (2020) used a digital PCR (dPCR) in replacement of a spectrophotometer to independently quantify stock standards used in the qPCR experiments. A droplet dPCR (ddPCR) was found to be able to quantify the diluted concentration of a stock standard with only 10% variation from the expected value, compared to spectrophotometric measurements which varied up to 98%.

This finding can revolutionize nucleic acid quantification and unify the interpretation of qPCR data, making it possible to make comparisons across laboratories and allow the qPCR results to speak the “same language.”

## ACKNOWLEDGEMENT

This work was supported by Cooperative Research Program for Agriculture Science and Technology Development (Project number: PJ014947022023) Rural Development Administration, Republic of Korea.

## REFERENCES

Ahn MS, Park PH, Kwon YN, Mekapogu M, Kim SW, Jie EY,

- Jeong JA, Park JT and Kwon OK.** (2018). Discrimination of floral scents and metabolites in cut flowers of Peony(*Paeonia lactiflora* Pall.) cultivars. *Korean Journal of Plant Resources*. 31:641-651.
- Beinhauerova M, Babak V, Bertasi B, Boniotti MB and Kralik P.** (2020). Utilization of digital PCR in quantity verification of plasmid standards used in quantitative PCR. *Frontiers in Molecular Biosciences*. 7:155. <https://www.frontiersin.org/journals/molecular-biosciences/articles/10.3389/fmolb.2020.00155/full>(cited by 2024 March 30).
- Cardin L, Onesto JP and Moury B.** (2010). First report of cucumber mosaic virus in *Paeonia lactifera* in France. *Plant Disease*. 94:790-790.
- Cheng Y, Kim CH, Shin DI, Kim SM, Koo HM and Park YJ.** (2011). Development of simple sequence repeat(SSR) markers to study diversity in the herbaceous peony(*Paeonia lactiflora*). *Journal of Medicinal Plants Research*. 5:6744-6751.
- Debat H and Bejerman N.** (2023). Two novel flavi-like viruses shed light on the plant-infecting kosovoviruses. *Archives of Virology*. 168:184. <https://link.springer.com/article/10.1007/s00705-023-05813-7> (cited by 2024 March 30).
- Fujimoto Y, Nijo T, Hosoe N, Watanabe K, Maejima K, Yamaji Y and Namba S.** (2018). Complete genome sequence of lychnis mottle virus isolated in Japan. *Genome Announcements*. 6:10.1128/genomea.00535-18. <https://journals.asm.org/doi/full/10.1128/genomea.00535-18> (cited by 2024 March 30).
- Gress JC, Smith S and Tzanetakis IE.** (2017). First report of Citrus leaf blotch virus in peony in the USA. *Plant disease*. 101:637-637.
- Igori D, Lee HK, Yang HJ, Lee DS, Kim SY, Kwon B, Oh J, Kim TD, An C, Moon JS and Lee SH.** (2020). First report of the cycas necrotic stunt virus infecting *Cnidium officinale* in South Korea. *Plant disease*. 104:3275-3275.
- Im I, Im BH, Park JH, Im MH, Jang JH and Lee IY.** (2017). Weed occurrence in peony(*Paeonia lactiflora*) fields. *Weed and Turfgrass Science*. 6:165-178.
- Jia A, Yan C, Yin H, Sun R, Xia F, Gao L, Zhang Y and Li Y.** (2021). Small RNA and transcriptome sequencing of a symptomatic peony plant reveals mixed infections with novel viruses. *Plant disease*. 105:3816-3828.
- Jiang P, Shao J and Nemchinov LG.** (2019). Identification of the coding-complete genome of cycas necrotic stunt virus in transcriptomic data sets of alfalfa (*Medicago sativa*). *Microbiology Resource Announcements*. 8:10.1128/mra.00981-19. <https://journals.asm.org/doi/full/10.1128/mra.00981-19> (cited by 2024 March 30).
- Jin W, Zhang Y, Su X, Wang R, Xie Z, Wang Y and Qiu Y.** (2023a). Development of colloidal gold immunochromatography and reverse-transcription loop-mediated isothermal amplification assays to detect lychnis mottle virus. *Plant disease*. 107:1584-1592.
- Jin W, Zhang Y, Su X, Xie Z, Wang R, Du Z, Wang Y and Qiu Y.** (2023b). Genetic diversity analysis of lychnis mottle virus and first identification of Angelica sinensis infection. *Heliyon*. 9:e17006. [chrome-extension://efaidnbmnnnibpcajpcglclefindmkaj/https://www.cell.com/heliyon/pdf/S2405-8440\(23\)04213-5.pdf](https://www.cell.com/heliyon/pdf/S2405-8440(23)04213-5.pdf) (cited by 2024 March 30).
- Kusunoki M, Hanada K, Iwaki M, Chang MU, Dol Y and Yora K.** (1986). Cycas necrotic stunt virus, a new member of nepoviruses found in *Cycas revoluta* host range, purification, serology and some other properties. *Japanese Journal of Phytopathology*. 52:302-311.
- Lim MY, Jana S, Sivanesan I, Park HR, Hwang JH, Park YH and Jeong BR.** (2013). Analysis of genetic variability using RAPD markers in *Paeonia* spp. grown in Korea. *Korean Journal of Horticultural Science and Technology*. 31:322-327.
- Lim S, Kwon SY, Lee JH, Cho HS, Kim HS, Park JM, Lee SH and Moon JS.** (2019). Genomic detection and molecular characterization of two distinct isolates of cycas necrotic stunt virus from *Paeonia suffruticosa* and *Daphne odora*. *Virus Genes*. 55:734-737.
- Lim SH, Han HS, Park JH and Lee J.** (2011). Methanol extract of peony root(*Peonia lactiflora*) and its ethyl acetate fraction attenuate heart and brain injury in a rat model of ischemia-reperfusion. *Journal of the Korean Society for Applied Biological Chemistry*. 54:799-801.
- Ochoa-Corona FM.** (2003). Detection of Cycas necrotic stunt virus (CNSV) in post-entry quarantine stocks of ornamentals in New Zealand. *Phytopathology*. 93:S67. <https://cir.nii.ac.jp/crid/1570854175402932096> (cited by 2024 March 30).
- Pfaffl WM.** (2004). Quantification strategies in real-time PCR. In: Bustin SA. (Ed.), *A-Z of Quantitative PCR*. International University Line (IUL), La Jolla, CA, USA. pp. 87-112.
- Robertson NL, Brown KL, Winton LM and Holloway PS.** (2009). First report of Tobacco rattle virus in Peony in Alaska. *Plant Disease*. 93:675-675.
- Shaffer CM, Gress JC and Tzanetakis IE.** (2019). First report of cycas necrotic stunt virus and lychnis mottle virus in peony in the United States. *Plant Disease*. 103:1048-1048.
- Shaffer CM, Michener DC, Vlasava NB, Chotkowski H, Botermans M, Starre J and Tzanetakis IE.** (2022a). First report of Gentian Kobu-sho-associated virus infecting peony in the United States and the Netherlands. *Plant Disease*. 106:1311. <https://apsjournals.apsnet.org/doi/full/10.1094/PDIS-06-21-1316-PDN> (cited by 2024 March 30).
- Shaffer CM, Michener DC, Vlasava NB, Chotkowski H, Lamour K, Stainton D and Tzanetakis IE.** (2021a). The population structure of the secovirid lychnis mottle virus based on the RNA2 coding sequences. *Virus Research*. 303:198468. <https://www.sciencedirect.com/science/article/abs/pii/S0168170221001751> (cited by 2024 March 30).
- Shaffer CM, Michener DC, Vlasava NB, Chotkowski H and Tzanetakis IE.** (2022b). Population genetics of cycas necrotic stunt virus and the development of multiplex RT-PCR diagnostics. *Virus Research*. 309:198655. <https://www.sciencedirect.com/science/article/abs/pii/S0168170221003622> (cited by 2024 March 30).
- Shaffer CM, Vakić M and Tzanetakis IE.** (2021b). First report of amazon lily mild mottle virus in peony in the United States. *Plant Disease*. 105:236. <https://apsjournals.apsnet.org/doi/full/10.1094/PDIS-04-20-0915-PDN> (cited by 2024 March 30).
- Smith CJ, Nedwell DB, Dong LF and Osborn AM.** (2006). Evaluation of quantitative polymerase chain reaction-based approaches for determining gene copy and gene transcript numbers in environmental samples. *Environmental Microbiology*.

8:804-815.

- Tang J, Ward L and Delmiglio C.** (2020). Occurrence of cycas necrotic stunt virus in *Paeonia lactiflora* in New Zealand. *Plant Disease*. 104:1567-1567.
- Uehara-Ichiki T, Nakazono-Nagaoka E, Ohashi M, Sato T, Hanada K, Tatsuo Y, Takao Y, Murakami Y, Kurosaki F, Aoki T and Fujikawa T.** (2016). Detection of several plant viruses from medical herbs, *Rehmannia glutinosa* varieties, and their nucleotide sequences. *Japanese Journal of Phytopathology*, 82:256. <https://cir.nii.ac.jp/crid/1370004235973018500> (cited by 2024 March 30).
- Uehara-Ichiki T, Ohashi M, Igarashi M, Hanada K and Hishida A.** (2020). Two plant viruses detected from Chinese peony (*Paeonia lactiflora* Pall.) in Japan. *Annual Report of the Kanto-Tosan Plant Protection Society*. 67:30-34.
- Wylie SJ, Luo H, Li H and Jones MGK.** (2012). Multiple polyadenylated RNA viruses detected in pooled cultivated and wild plant samples. *Archives of Virology*. 157:271-284.
- Yoo RH, Zhao F, Lim S, Igori D, Lee SH and Moon JS.** (2015). The complete nucleotide sequence and genome organization of lychnis mottle virus. *Archives of Virology*. 160:2891-2894.
- Yoon JY, Soeng C, Ju HJ, Cho IS and Chung BN.** (2024). First report of cycas necrotic stunt virus in a hybrid peony in South Korea. *Journal of Plant Pathology*. 106:761-762.
- Yu SJ.** (1970). Anatomical studies on the classification of the cultivated peony in Korea. *Korean Journal of Pharmacognosy*. 1:81-92.
- Yue M, Li S, Yan G, Li C and Kang Z.** (2018). Paeoniflorin inhibits cell growth and induces cell cycle arrest through inhibition of FoxM1 in colorectal cancer cells. *Cell Cycle*. 17:240-249.